Evolutionary Stalling in the Optimization of the Translation Machinery

Sandeep Venkataram[1], Ross Monasky[2], Shohreh H Sikaroodi[1,3], Sergey Kryazhimskiy[1,*,†], Betül Kaçar[2,*,†]

[1]Division of Biological Sciences, University of California San Diego, La Jolla, CA 92093;
[2]Department of Molecular and Cellular Biology, University of Arizona, Tucson, AZ 85721;
[3]Current address: Molecular engineering group, Fate Therapeutics Inc.
[*]Equal contribution
[†]Corresponding authors: betul@arizona.edu, skryazhi@ucsd.edu

Abstract

Biological organisms are modular. Theory predicts that natural selection would steadily improve modules towards their performance optima up to the margin of effective neutrality. This classical theory may break down for populations evolving in the clonal interference regime because natural selection may focus on some modules while adaptation of others stalls. Such evolutionary stalling has not been observed and it is unclear whether it limits the power of natural selection to optimize module performance. To empirically characterize evolutionary stalling, we evolved populations of *Escherichia coli* with genetically perturbed translation machineries (TMs). We show that populations with different suboptimal TMs embark on statistically distinct trajectories of TM optimization. Yet, before TMs approach the margin of effective neutrality, the focus of natural selection shifts to other cellular modules, and TM optimization stalls. Our results suggest that module optimization within an organism may take much longer than suggested by classical theory.

Introduction

Biological systems are organized hierarchically, from molecules to cells, organisms and populations [1–5]. At the lowest level, molecules within cells form functional modules, such as the translation machinery, or various other metabolic pathways [4,6–9]. Organismal fitness depends on the performance of these modules. However, the ability of natural selection to optimize cellular modules is constrained by the abundance and the effects of available beneficial mutations.

In the simplest case, the speed of evolutionary optimization of a module depends only on the supply and the fitness effects of beneficial mutations in that module. Theoretical models predict that the fitness effects of beneficial mutations will decline as the module's performance approaches an optimum. Therefore, the module's performance is expected to improve steadily, albeit with a gradually declining rate [10–21]. When the module's performance approaches the optimum and the fitness effects of beneficial mutations drop below ~1/N, the inverse of the population size, the optimization of the module by natural selection stops [12,22–24].

In reality, evolution of any one module within an organism depends on the supply and effects of beneficial mutations in all modules. One reason for this interdependence is that modules are encoded in genomes, and genomes are physically linked [25]. Therefore, new beneficial mutations affecting different modules must compete against each other in the population whenever they simultaneously arise on different genetic backgrounds [25–29]. This effect, known as "clonal interference", is particularly strong when recombination is rare and the supply of adaptive mutations is large [25,28], e.g., if the organism reproduces asexually, the population is large and the environment is new. In the clonal interference regime, small-effect mutations are usually outcompeted. Instead, adaptation is driven by mutations that provide fitness benefits above a certain "clonal interference" threshold, which depends on the current supply and the fitness effects of all adaptive mutations in the genome [25,29,30].

Beneficial mutations in different modules likely arise at different rates and have different effects on the fitness of the organism. Therefore, natural selection will be "focused" on optimizing modules where mutations have effects above the clonal interference threshold, while other modules would adapt slowly or not at all. Modules that are more important for fitness in the current environment and those that are farther from their performance optima are expected to contribute more large-effect mutations. Such modules are more likely to be in the focus of natural selection. However, as natural selection improves the performance of any such module, the supply and effects of adaptive mutations in that module will decline. Eventually, further improvements will only be possible by mutations with effects below the clonal interference threshold. At this point, the evolutionary optimization of the focal module will slow down or cease entirely. We call this phenomenon "evolutionary stalling".

Evolutionary stalling imposes a limit on the power of natural selection to improve the performance of a module within an organism, in addition to the well known threshold of effective neutrality. While the effective neutrality threshold cannot be overcome, evolutionary optimization of a stalled module can resume once large-effect adaptive mutations in competing modules are exhausted. Nevertheless, stalling poses a potentially serious obstacle for the evolutionary optimization of a module because it can occur much farther from the optimum than the hard limit of effective neutrality.

The onset of evolutionary stalling has never been directly observed. Experiments in microbes show that the conditions for the onset of stalling are generally favorable. First, microbial populations usually evolve in the clonal interference regime [26,31–35]. Second, when healthy strains adapt to benign laboratory conditions, multiple different cellular processes are affected by beneficial mutations, which suggests that multiple modules can be potentially improved by natural selection [32,36–41]. On the other hand, when an important cellular module is genetically disrupted or the environment is harsh, natural selection is focused on a single module [38,39,41–50]. In these cases, once the poorly performing module is sufficiently improved, we expect that its further optimization would eventually stall, and the focus of natural selection would shift to other modules that are still suboptimal. This transition in the focus of selection has not been characterized. In particular, it remains unknown how close to the performance optimum natural selection is able to push an initially defective module before the onset of stalling.

Evolutionary stalling can be detected in two ways. If we can directly measure the performance of a module over time, an abrupt reduction in the rate of its phenotypic improvement despite steady increases in fitness would potentially indicate the onset of stalling. Alternatively, if we know all the genes that encode a module, we could potentially infer the onset of stalling from an abrupt reduction in the rate of accumulation of mutations in such genes despite continued accumulation of beneficial mutations elsewhere in the genome. Both approaches are challenging because it is often unclear what aspects of a module's performance are relevant for fitness and because in general the location of the performance optima and the identities of all genes that encode modules are unknown.

Here, we experimentally examine the evolution of the translation machinery (TM), one of the best annotated and characterized cellular modules [8,9,51–53]. This choice allows us to use the genomic approach for detecting evolutionary stalling. Extant TMs are unique in that they are close to their theoretical performance optimum [54], which allows us to estimate how far from the margin of effective neutrality stalling occurs. We disrupted the TM by replacing the native translation Elongation Factor Tu (EF-Tu) in the bacterium *Escherichia coli* (*E. coli*) with its orthologs [55–57]. We then evolved these strains in rich media where rapid and accurate translation is required for fast growth [58,59]. We expect that natural selection will favor mutations that repair the initial TM defects. We characterize the onset of evolutionary stalling in the TM in two ways. First, we observe substitutions in known TM genes only in strains with the most severe initial TM defects and quantify how far from the optimum stalling occurs. Second, we observe that mutations in TM genes are exhausted within evolving populations, which provides us with direct evidence for the onset of evolutionary stalling.

Results

We previously replaced the native EF-Tu in *E. coli* with its orthologs from *Salmonella typhimurium*, *Yersinia enterocolitica*, *Vibrio cholerae* and *Pseudomonas aeruginosa* and one reconstructed ancestral variant [55] (Table 1). EF-Tu is encoded in *E. coli* by two paralogous genes, *tufA* and *tufB*, with the majority of the EF-Tu molecules being expressed from *tufA* [60]. To replace all EF-Tu molecules in the cells, the *tufB* gene was deleted and the foreign orthologs were integrated into the *tufA* locus [55]. We also included the control strain in which the *tufB* gene was deleted and the original *E. coli tufA* was left intact. We refer to the engineered "founder" *E. coli* strains as E, S, Y, V, A and P by the first letter of the origin of their *tuf* genes (Table 1).

Strain	EF-Tu origin species	Number of amino acid differences from *E. coli* EF-Tu (percent identity)	Fitness ± SEM, % per generation
E	*Escherichia coli* (control)	0 (100)	0 ± 0.7
S	*Salmonella typhimurium*	1 (99.75)	+0.49 ± 0.09
Y	*Yersinia enterocolitica*	24 (93.91)	–3.02 ± 0.03
V	*Vibrio cholerae*	51 (87.06)	–19.0 ± 1.1
A	Reconstructed ancestor	21 (94.67)	–34.4 ± 0.7
P	*Pseudomonas aeruginosa*	62 (84.38)	–35.0 ± 0.2

Table 1. Founders used for the evolution experiment. Strains with foreign EF-Tu orthologs are ordered by their fitness relative to the control E strain. SEM stands for standard error of the mean.

We first quantified the sub-optimality of the TMs in our founder strains. Kaçar et al. showed that EF-Tu replacements lead to declines in the *E. coli* protein synthesis rate and proportional losses in growth rate in the rich laboratory medium LB [55]. In our subsequent evolution experiment, natural selection will favor genotypes with higher competitive fitness, which may have other components in addition to growth rate [61–65]. We confirmed that EF-Tu replacements caused changes in competitive fitness relative to the control E strain (Table 1), and that competitive fitness and growth rate were highly correlated (Figure S1). We conclude that the competitive fitness of our founders in our environment reflects their TM performance. The fitness of the S and Y founders were similar to that of the control E strain (≤ 3% fitness change) indicating that their TMs were at most mildly suboptimal. In contrast, the fitness of the V, A and P founders were dramatically lower (≥ 19% fitness decline; Table 1) indicating that their TMs were severely suboptimal.

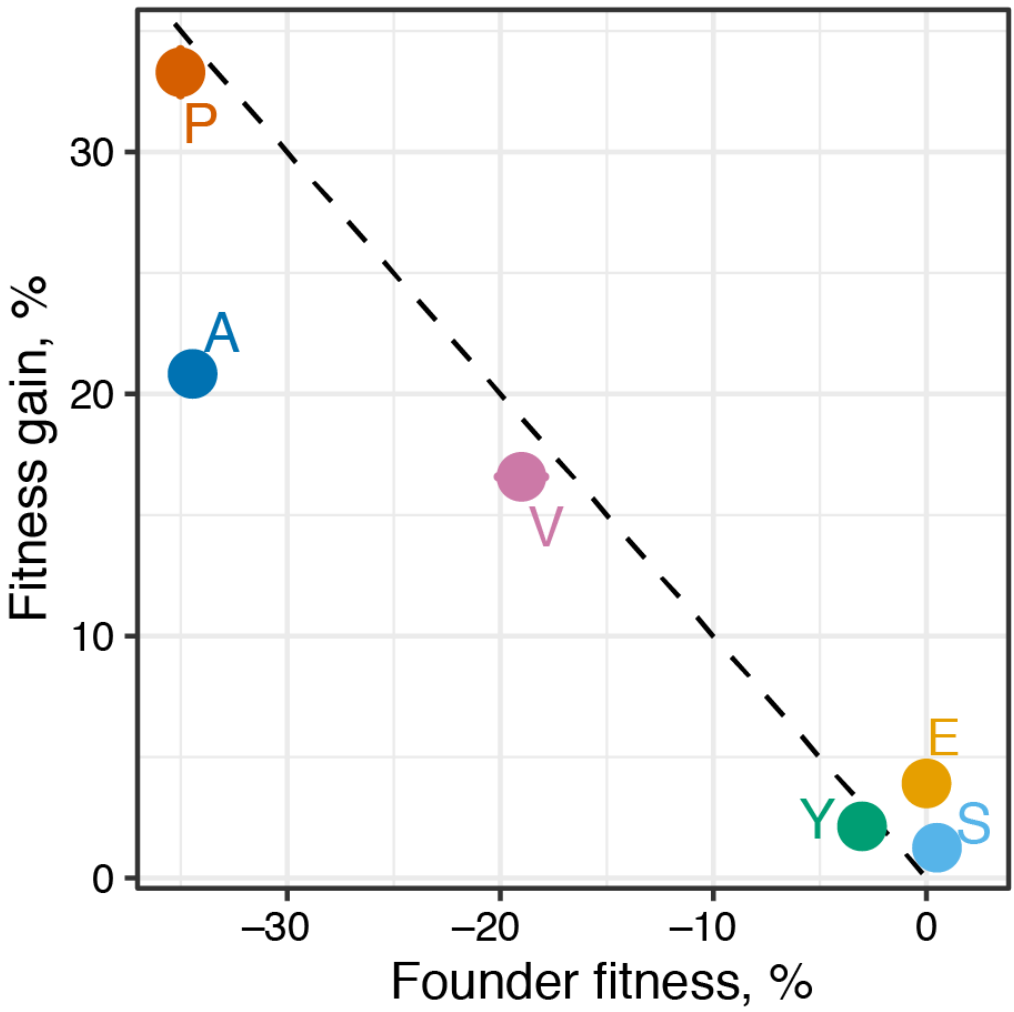

Figure 1. Competitive fitness of founder and evolved populations. The competitive fitness gain after evolution relative to the unevolved founder averaged across replicate populations (*y* axis) is plotted against the competitive fitness of the founder relative to the E strain (*x* axis). Fitness is measured in % per generation. Dashed black line is $y = -x$. Populations above (below) this line are more (less) fit than the control E strain, under the assumption that fitness is transitive. Error bars showing ±1 SEM are masked by the symbols (see Table 1 and Figure S2).

Clonal interference inhibits the ability of natural selection to optimize the TM

To determine whether natural selection focuses on restoring defective TMs, we instantiated 10 replicate populations from each of our six founders (60 populations total) and evolved them in LB for 1,000 generations (Methods) with the bottleneck population size $N = 5\times10^5$ cells. We then measured the competitive fitness of the evolved populations relative to their respective founders. Fitness in all but one population increased significantly (t-test $P < 0.05$ after Benjamini-Hochberg correction; Figure S2), and the average fitness increase of a population correlated negatively with the initial fitness of its founder (Figure 1). These results show that even

142 substantial fitness defects caused by reductions in TM performance can be largely compensated
143 in a short bout of adaptive evolution.

144 The pattern of "declining adaptability" in Figure 1 has been frequently observed in previous
145 microbial evolution studies [37,39,41,66–70]. It could arise if adaptation is driven either by
146 mutations only in the TM, by mutations only in other modules, or by mutations in the TM and in
147 other modules. For evolutionary stalling in the TM to occur, mutations improving the TM must
148 compete against other types of mutations within the same population. To determine whether both
149 types of mutations occur in our populations, we conducted whole-population whole-genome
150 sequencing at multiple timepoints throughout the evolution experiment. This sequencing strategy
151 allows us to directly observe competition dynamics between mutations in different modules
152 [32,34,35,40].

153 We selected replicate populations 1 through 6 descended from each founder (a total of 36
154 populations), sampled each of them at 100-generation intervals (a total of 11 time points per
155 population) and sequenced the total genomic DNA extracted from these samples. We developed
156 a bioinformatics pipeline to identify de novo mutations in this data set (Methods). Then, we
157 called a mutation adaptive if it satisfied two criteria: (i) its frequency changed by more than 20%
158 in a population; and (ii) it occured in a "multi-hit" gene, i.e., a gene in which two independent
159 mutations passed the first criterion. Reliably tracking the frequencies of some types of mutations
160 (e.g., large copy-number variants) is impossible with our sequencing approach. Therefore, we
161 augmented our pipeline with the manual identification of copy-number variants which could only
162 be reliably detected after they reached high frequency in a population (Methods and Figure S3).

163 This procedure yielded 167 new putatively adaptive mutations in 28 multi-hit genes, with the
164 expected false discovery rate of 13.6%, along with an additional 11 manually-identified
165 chromosomal amplifications, all of which span the *tufA* locus (Methods and Table S1, Figure
166 S4). We classified each putatively adaptive mutation as "TM-specific" if the gene where it
167 occurred is annotated as translation-related (Methods). We classified mutations in all other genes
168 as "generic". We found that 38 out of 178 (21%) putatively adaptive mutations in 6 out of 28
169 multi-hit genes were TM-specific (Table S1). This is significantly more mutations than expected
170 by chance ($P < 10^{-4}$, randomization test) since the 215 genes annotated as translation-related
171 comprise only 4.0% of the *E. coli* genome. All of the TM-specific mutations occurred in genes
172 whose only known function is translation-related, such as *rpsF* and *rpsG*, suggesting these
173 mutations arose in response to the initial defects in the TM. The set of TM-specific mutations is
174 robust with respect to our filtering criteria (Figure S5).

175 TM-specific mutations occurred in 17 out of 36 sequenced populations. Generic mutations were
176 also observed in all of these populations (Figure S4). Thus, whenever TM-specific mutations
177 occurred, generic mutations also occurred, such that the fate of TM-specific mutations must have
178 depended on the outcome of clonal interference between mutations within and between modules
179 (Figure 2). As a result of this competition, only 14 out of 27 (52%) TM-specific mutations that
180 arose (excluding 11 *tufA* ampliciations) went to fixation, while the remaining 13 (48%)
181 succumbed to clonal interference (Figures 2, S4). In at least two of these 13 cases a TM-specific
182 mutation was outcompeted by expanding clones likely driven by generic mutations: in
183 population V6, a TM-specific mutation in *fusA* was outcompeted by a clone carrying generic
184 mutations in *fimD*, *ftsI* and *hslO* (Figure 2); in population P3, a TM-specific mutation in *tufA* was
185 outcompeted by a clone carrying generic mutations in *amiC* and *trkH* (Figure 2). We conclude
186 that, while TM-specific beneficial mutations are sufficiently common and their fitness effects are

at least sometimes large enough to successfully compete against generic mutations, clonal interference reduces the power of natural selection to re-optimize the TM.

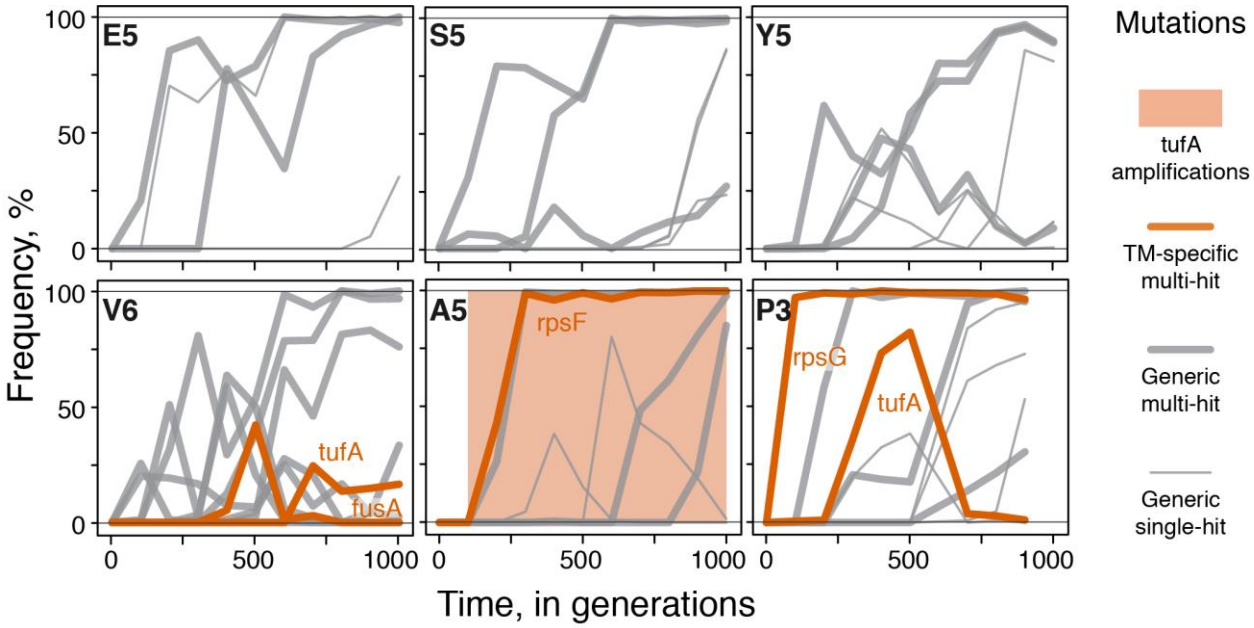

Figure 2. Mutational trajectories in evolving populations. Mutation frequency trajectories for one representative replicate population per founder is shown (complete data for all sequenced populations can be found in Figure S4). Each line represents the frequency trajectory of a single mutation. Shading indicates the range of timepoints in which a *tufA* amplification was detected.

Evolution of the TM stalls far from the optimum

Competition between adaptive mutations in different modules is necessary but not sufficient for evolutionary stalling to occur in any one module. Therefore, we sought direct evidence of evolutionary stalling in the TM. To this end, we examined the distribution of TM-specific mutations among founders and across evolutionary time. All of the detected TM-specific mutations occurred in the V, A and P populations whose TMs were initially severely suboptimal; no TM-specific mutations were detected in the E, S, and Y populations whose TMs were mildly suboptimal (Figure 3A). Out of the 14 TM-specific mutations that eventually fixed in the V, A and P populations, 12 (86%) did so in the first selective sweep (this excludes 11 *tufA* amplifications). In contrast, out of the 16 generic mutations that fixed in these populations, only 7 (44%) did so in the first selective sweep. As a result, an average TM-specific beneficial mutation reached fixation after only 300 ± 52 generations, compared to 600 ± 72 generations for an average generic mutation (Figure 3B, S4). Only one (7%) TM-specific beneficial mutation reached fixation after generation 600, in comparison to 9 (56%) generic beneficial mutations. Thus, by the end of our evolution experiment, adaptive TM-specific mutations are depleted even in populations descended from the V, A and P founders.

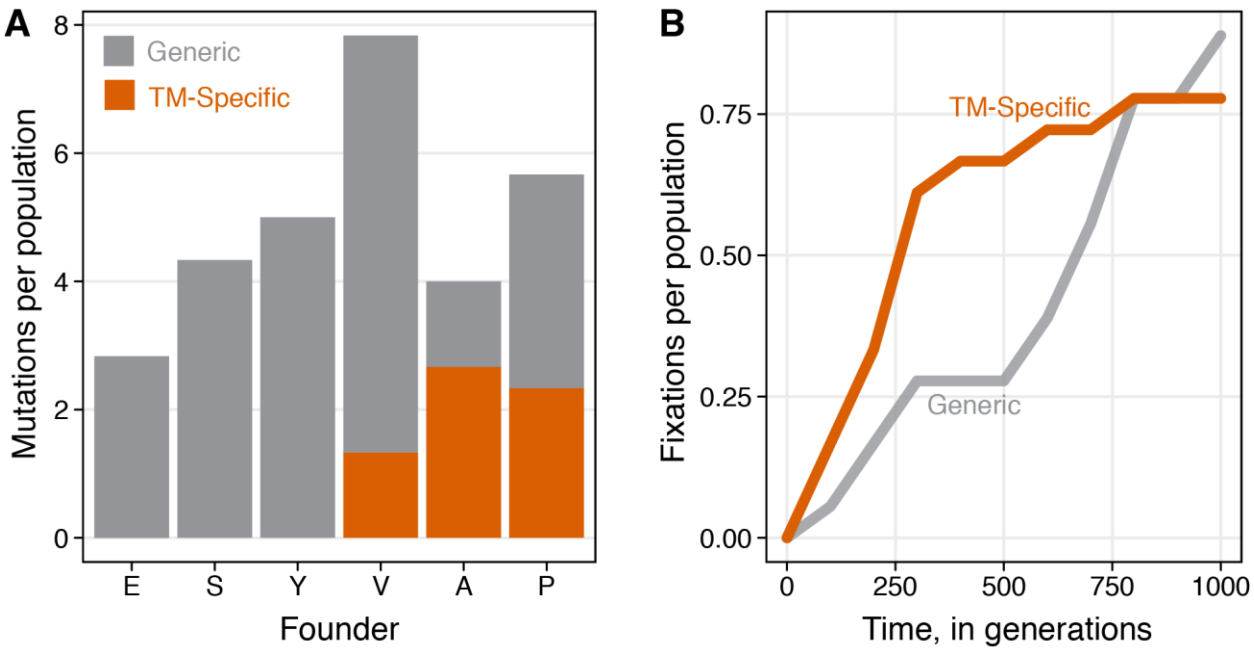

Figure 3. Evidence for stalling in the evolutionary optimization of the TM. A. Number of adaptive TM-specific and generic mutations identified in the six sequenced populations derived from each of the founders. **B.** Cumulative number of fixed TM-specific or generic mutations per population derived from the V, A and P founders.

These data demonstrate that evolutionary stalling in the optimization of the TM occurs in our populations. They also allow us to place bounds on the TM defects which can and cannot be improved by natural selection prior to the onset of evolutionary stalling. First, consider the founder Y in which the initial defect in the TM incurs a ~3% fitness cost (Table 1). While Y populations gained on average 2.4% in fitness during evolution (Figure 1), none of these gains are attributed to TM-specific mutations. This indicates that TM adaptation is stalled if the initial TM defect incurs $\leq 3\%$ fitness cost. Next, consider founder V in which the initial defect in the TM incurs a ~19% fitness cost (Table 1). We observed 8 TM-specific mutations across all V populations, including three *tufA* amplifications. At least one of these mutations reached fixation (Figure S4), suggesting that natural selection can repair defects in the TM that incur $\geq 19\%$ fitness cost without the onset of evolutionary stalling. We conclude that the focus of natural selection shifts from optimizing the TM to other cellular modules when the TM incurs a fitness cost somewhere between 3% and 19%.

Another way of arriving at a lower bound for the onset of stalling is to consider the V, A and P populations. On average, these populations fixed 0.8 TM-specific mutations during evolution, and remained ~5.3% less fit than the control E strain, assuming fitness is transitive (Figure 1). Even if we conservatively attribute all these fitness gains to improvements in the TM, by the end of the experiment, TMs in these populations must still be on average ~5.3% below the optimum. Yet, by the end of the experiment, fixation of TM mutations had essentially stopped, while fixation of generic mutations continued unabated (Figures 3B). This suggests that TMs that incur fitness defects larger than 3% may still be subject to evolutionary stalling.

To further corroborate and possibly refine these bounds, we selected two TM-specific mutations that arose in our populations, genetically reconstructed them in their respective founder strains and directly measured their fitness benefits. The TM-specific mutation A74G in the *rpsF* gene,

which arose in population A5, provides an 8.2 ± 1.0% fitness benefit in the A founder. The TM-specific mutation G331A in gene *rpsG*, which arose in populations P2, P3 and P5, provides a 6.5 ± 1.2% fitness benefit in the P founder. Such large-effect mutations can never arise in TMs that incur a less than 6.5% fitness cost, which is further indirect evidence that TM adaptation stalls when it incurs a fitness cost larger than our conservative 3% bound.

If the TM was the only suboptimal module in the cell, theory suggests that its adaptation would continue until the fitness defect it incurs is $\frac{n-1}{8N}$, where n is the effective number of TM phenotypes relevant for fitness and N is the population size [12]. Although n is unknown, it is typically thought to be small, even for entire organisms [18,71]. Assuming that $n \lesssim 10^3$, which seems reasonable given that there are roughly 215 translation-related genes in *E. coli* (Methods), the effective neutrality threshold is $\lesssim 0.025\%$. As the TM is not the only module that natural selection needs to optimize, its adaptation stalls orders of magnitude above the theoretically predicted effective neutrality threshold.

Epistasis and historical contingency in TM evolution

We observed that natural selection improved all severely suboptimal TMs, but it is unclear whether different TM defects can be alleviated by a common set of mutations or whether repairing each TM defect requires its own unique solution. Previous work has shown that genetic interactions (or "epistasis") between mutations in the TM have been important in the evolutionary divergence of TMs along the tree of life [55,72–75]. We reasoned that genetic interactions might be similarly important in the short bout of evolution observed in our experiment. Specifically, we asked whether different initial TM variants acquired adaptive mutations in the same or in different translation-associated genes.

We found that 4 out of 7 classes of TM-specific mutations arose in a single founder (Figure 4A). For example, we detected six independent mutations in the *rpsG* gene, which encodes the ribosomal protein S7, and all of these mutations occurred in the P founder ($P < 10^{-4}$, randomization test with Benjamini-Hochberg correction, Methods). Similarly, all four mutations in the *rpsF* gene, which encodes the ribosomal protein S6, occurred in the A founder ($P < 10^{-4}$, randomization test with Benjamini-Hochberg correction). To directly measure how the effects of these mutations vary across genetic backgrounds, we attempted to genetically reconstruct mutation A74G in the *rpsF* gene and mutation G331A in *rpsG* gene in all six of our founder strains. We successfully reconstructed both of these mutations in the founder strains in which they arose and confirmed that they were strongly beneficial, as described above (8.2 ± 1.0% and 6.5 ± 1.2% benefit, respectively). In contrast, our multiple reconstruction attempts in all other founders were unsuccessful (Methods), suggesting that these mutations are strongly deleterious in all other genetic backgrounds that we tested.

These results suggest that genetic interactions between different TM components cause initially different TM variants to embark on divergent adaptive trajectories and lead to historical contingency and entrenchment in TM evolution [76–78].

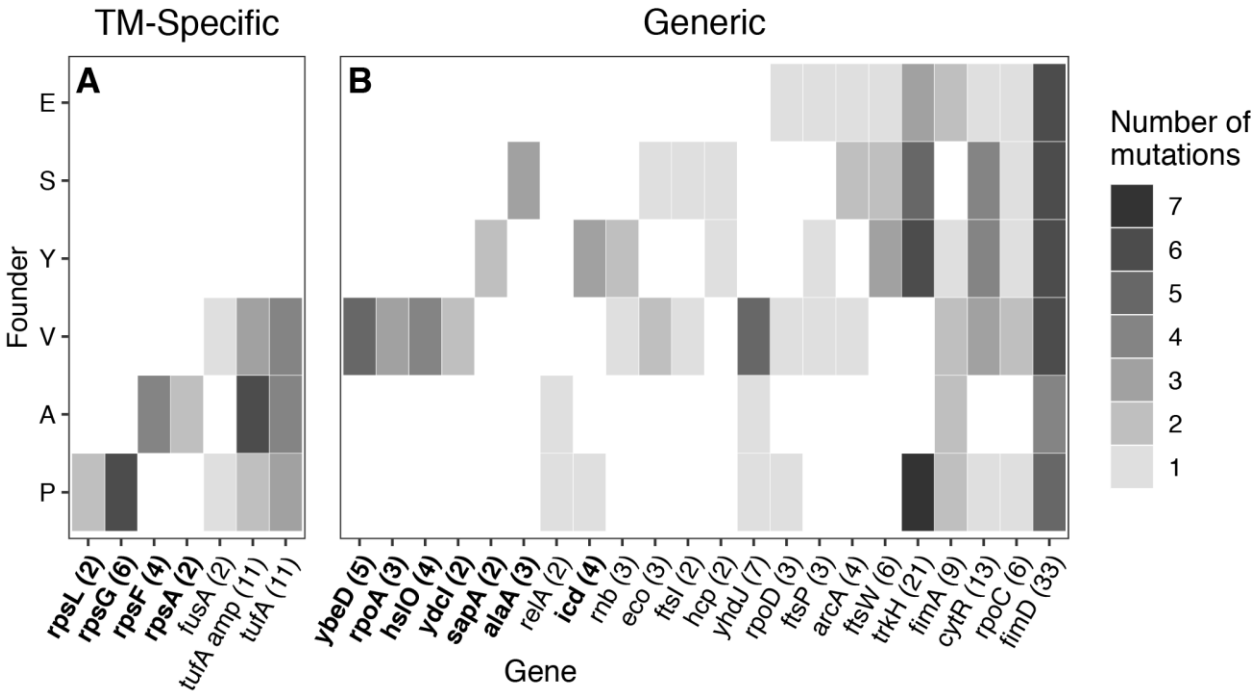

Figure 4. Distribution of putatively adaptive mutations. Heatmap of all putatively adaptive mutations identified via whole-genome sequencing, grouped by founder and by gene. Amplification of the *tufA* locus are counted separately from other mutations in *tufA*. **A.** Translation-associated genes **B.** All other genes. Genes in bold are those where mutations were detected in significantly fewer founders than expected by chance ($P < 0.05$, Benjamini-Hochberg correction, see Methods). Numbers in parentheses indicate the total number of mutations in that gene observed across all sequenced populations.

Genome-wide adaptive responses to TM perturbations

Adaptive evolution of the TM stalls because natural selection acts on multiple cellular modules in *E. coli*, all of which are encoded on a single non-recombining chromosome. However, modules are linked not only physically by the encoding DNA but also functionally in that they all contribute to the fitness of the organism. This functional interdependence implies that mutations in one module may alter the selection pressure on other modules. For example, improvements in translation efficiency may increase the selection pressure to improve efficiency of catabolic reactions, analogously to the "shifting and swaying of selection coefficients" on enzymes in the same metabolic pathway discussed in the classic work by Hartl et al. [22]. Therefore, in addition to intra-module epistasis demonstrated above we might expect inter-module epistasis, such that initially different TM variants could precipitate distinct adaptive responses in the rest of the genome. To test this hypothesis, we examined the distribution of generic mutations among founder genotypes.

We found that generic mutations in 7 out of 22 genes occurred in fewer founders than expected by chance (Figure 4B, Methods). For example, we detected five independent mutations in the *ybeD* gene, which encodes a protein with an unknown function, and all these mutations occurred in the V founder ($P < 10^{-4}$, randomization test with Benjamini-Hochberg correction). Similarly, all three mutations in the *alaA* gene, which encodes a glutamate-pyruvate aminotransferase, occurred in the A founder ($P < 10^{-4}$, randomization test with Benjamini-Hochberg correction). To corroborate these statistical observations, we reconstructed the T93G mutation in the *ybeD*

gene in all six founder strains and directly measured its fitness effects. As expected, this mutation confers a 5.9% fitness benefit in the V founder. In contrast, it is strongly deleterious in the P founder and indistinguishable from neutral in the remaining founders (Figure 5). These results show that at least some genetic perturbations in the TM can have genome-wide repercussions. They can precipitate bouts of genome-wide adaptive evolution that are contingent on the initial perturbations in the TM.

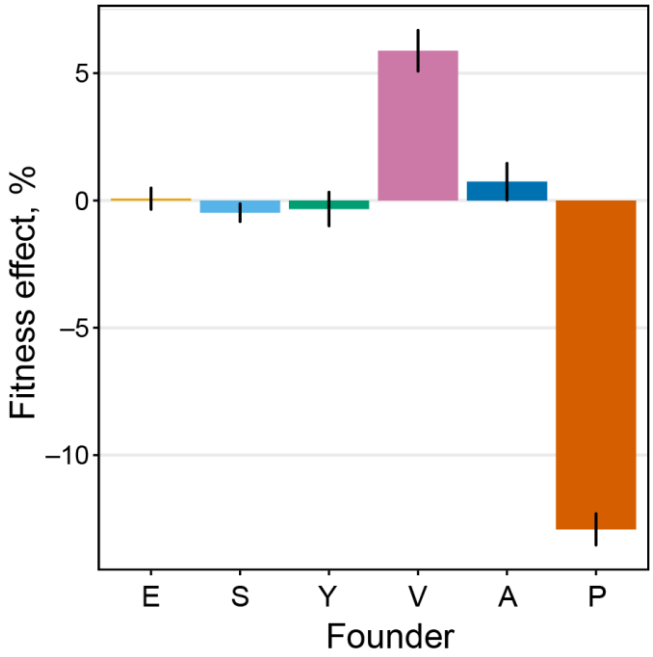

Figure 5. Fitness effect of the *ybeD* T193D mutation in different founders. Fitness effect of the mutation is measured in a direct competition of each founder with the mutation against the founder without the mutation. Error bars show the SEM.

Discussion

The fitness of an organism depends on the performance of many molecular modules inside cells. While natural selection favors genotypes with better-performing modules, it is difficult for evolution to optimize multiple modules simultaneously, particularly when recombination rates are low and many adaptive mutations in different modules are available. In this regime, natural selection is expected to focus on optimizing those modules where many mutations provide large fitness benefits, while the adaptive evolution in other modules stalls. Here we have documented and characterized the evolutionary stalling of the translation machinery (TM) in *E. coli*.

We found that evolutionary optimization of the TM was slowed down by competition with adaptive mutations in the rest of the genome (Figure 2). The populations whose TMs were initially mildly sub-optimal (incurring $\lesssim 3\%$ fitness cost) adapted by acquiring mutations that did not directly affect the TM. In contrast, populations whose TMs were initially severely sub-optimal (incurring $\gtrsim 19\%$ fitness cost) rapidly discovered and fixed TM-specific beneficial mutations. We conclude that the adaptive evolution of the TM stalls when the TM defect incurs a fitness cost between 3% and 19%. This is a conservative lower bound on the onset of stalling that we derived under the assumption that the TM in the control E strain is close to optimal. However, the E strain itself suffers a $4.1 \pm 0.1\%$ fitness defect relative to wild-type *E. coli* that contains the *tufB* gene (Methods). Thus, the adaptive evolution of the TM may actually stall when the TM defect incurs a fitness cost between 7.1% and 23.1%.

Evolutionary stalling in the TM occurs for one of two reasons. First, the rate of TM-specific beneficial mutations may be too low for these mutations to survive genetic drift when rare. Alternatively, these mutations occur frequently enough to survive drift but succumb to clonal interference. Both theoretical and empirical (albeit limited) evidence suggest that small-effect beneficial mutations are more common than large-effect mutations [16,19,79,80]. The fact that we observed TM-specific mutations with effects $\geq 5\%$ indicates that the rate of such mutations is high. We expect the rate of TM-specific mutations with effects $< 5\%$ to be even higher. If we relax the stringency criteria for detecting beneficial mutations, we find one TM-specific mutation in the gene *rbbA* in the population E5 (Figure S5). This suggests that small-effect TM-specific beneficial mutations exist and supports the conjecture that adaptation of the TM stalls because of clonal interference.

Our results show that evolutionary stalling limits the ability of natural selection to improve a module, but this limit is not absolute. As a population accumulates beneficial mutations in other modules, their supply will be depleted and their fitness effects will likely decrease due to diminishing returns epistasis [37,66,67,81–83]. These changes will in turn increase the chances for small-effect mutations in the focal module to survive clonal interference thereby overcoming evolutionary stalling. While we did not observe resumption of adaptive evolution in the TM in this experiment, we find some evidence for such a transition in one other module. We detected 11 mutations in multi-hit genes that affect cytokinesis (Methods, Figures S6, S7). Most of these mutations reached high frequency in the second half of the experiment, suggesting that adaptation in the cytokinesis module was initially stalled and then resumed.

General implications for the evolution of modular systems

Evolutionary stalling can occur much farther from the optimum than the margin of effective neutrality, which poses a potentially serious obstacle for evolutionary optimization, in particular when selection pressures vary over time. To overcome evolutionary stalling in a module, the supply of large-effect beneficial mutations in other modules must be depleted. However, variability in selection pressures can replenish this supply, leaving the focal module stalled far from the optimum. Thus, long periods of time under constant selection pressures might be required for natural selection to fully optimize even essential modules.

Our results imply that it is impossible to fully understand the evolution a cellular module in isolation from the genome where it is encoded and the population-level processes that govern evolution. The ability of natural selection to optimize any one module depends on the population size, the rate of recombination, the supply and the fitness effects of all beneficial mutations in the genome and on how these quantities change as the population adapts. Further theoretical work and empirical measurements integrated across multiple levels of biological organization are required for us to understand adaptive evolution of modular biological systems.

Implications for the evolution the translation machinery

In this work, we identified several TM-specific adaptive mutations, but their biochemical and physiological effects are at this point unknown. However, the fact that 11 chromosomal amplifications and 12 noncoding or synonymous events occurred in the *tufA* operon suggests that some of the TM-specific mutations are beneficial because they adjust EF-Tu abundance in the cell. This would be consistent with previous evolution experiments [46,84,85]. Directly measuring the phenotypic effects of the TM-specific mutations described here is an important avenue for future work.

Our results give us a glimpse of the fitness landscape of the TM. This landscape is broadly consistent with Fisher's geometric model in that the distribution of fitness effects of beneficial mutations depends on the distance to the performance optimum [10,16,21]. However, Fisher's model does not inform us how many distinct genotypes encode this optimum and how they are connected in the genotype space. We observed that evolutionary trajectories originating at different initial defective TMs gained distinct TM-specific adaptive mutations. This suggests that the TM performance optimum is encoded by multiple genotypes that either form a single contiguous neutral network [86] or multiple isolated neutral networks [87]. Moreover, we observed that most of our populations with initially severely suboptimal TMs were able to discover TM-specific mutations. This suggests that genotypes that encode high-performing TMs may be present in the mutational neighborhoods of many genotypes [86,88].

How did the translation machinery historically evolve on this fitness landscape? Extant TMs are thought to be nearly optimal [54], but when and how TMs evolved to this optimal state is unknown. Our work helps us constrain the plausible evolutionary scenarios. One possibility is that the TM approached the optimum prior to the last universal common ancestor (LUCA), and subsequent evolution in TM components along most lineages was driven by conditionally neutral and mildly deleterious substitutions. Another possibility is that the TM in LUCA was not optimal, and TMs in different lineages were optimized after LUCA. Our results suggest that evolving an optimal TM after it was encapsulated in a cell with a physically contiguous genome

may have been difficult, especially if other components of the cell also required continuous adaptation to a changing environment. In other words, the possibility that the TM has been functionally optimized prior to LUCA appears more likely.

Materials and methods

Materials, data and code availability

All strains and plasmids constructed and used in this work are available per request. Raw sequencing data were analyzed with the python-based workflow implemented in Ref. [40] and run on the UCSD TSCC computing cluster via a custom python wrapper script. All analysis and plots reported in this manuscript have been performed using the R computing environment. The script, modified reference genomes and the raw data (except for raw sequencing data) used for analysis can be found at https://github.com/sandeepvenkataram/EvoStalling. Raw sequencing data for this project have been deposited into the NCBI SRA under project PRJNA560969.

Media and culturing conditions

Liquid medium is the Luria-Bertani medium (LB) (per liter, 10 g NaCl, 5 g yeast extract, and 10 g tryptone) and solid medium is LBA (LB with 1.5% agar), unless noted otherwise. All incubations were done at 37°C, and liquid cultures were shaken at 200 rpm for aeration, unless noted otherwise. All media components and chemicals were purchased from Sigma, unless noted otherwise.

Strains and plasmids

All strains in this study were derived from *E. coli* K12 MG1655. Strain genotypes are listed in Table S2. Complete methods for the construction of the E, S, Y, V, A and P strains, which harbor a single *tuf* gene variant replacing *tufA* gene, can be found in Ref. [55]. Strains with engineered *ybeD*, *rpsF* and *rpsG* mutations were constructed using the same method, except the chromosomal *kanR* marker was not removed (Figure S9). For a full list of primer sequences used for *ybeD*, *rpsF* and *rpsG* engineering, see Table S2.

Plasmids pZS1-TnSL and pZS2-TnSL were used in competition assays to provide Ampicillin and Kanamycin resistance, respectively. pZS1-TnSL, derived from pUA66 [89], was kindly provided by Georg Rieckh. pZS2-TnSL was constructed from pZS1-TnSL by replacing the *ampR* cassette with *kanR*.

Evolution experiment

Experimental evolution was performed by serial dilution at 37°C in LB broth. To start the evolution experiment, an initial 5 mL overnight culture was inoculated from a single colony from the frozen stock of each founder strains. 10 replicate populations were started from single colonies derived from these overnight cultures. The replicates were serially transferred every 24h (±1h) as follows: 100 µL of saturated culture were transferred into 10 mL saline solution (145 mM NaCl), 50 µL of these dilutions were then transferred to 5 mL fresh LB (tubes were vigorously vortexed prior to pipetting). This resulted in a bottleneck population size of about 5×10^5 cells. Freezer stocks (200 µL of 20% glycerol + 1 mL saturated culture) were prepared approximately every 100 generations and stored at –80°C.

Competitive fitness assays

To carry out pairwise competition assays, an Ampicillin-resistant and a Kanamycin-resistant versions of the query and reference strains/populations were generated by transforming these strains/populations with plasmids pZS1-TnSL and pZS2-TnSL, using standard methods [90]. Two replicate competition assays were performed for each query-reference pair with reciprocal markers (four assays total per pair), except for allele-replacement mutants (see below). To validate that the resistance-marker plasmids do not differentially impact fitness in any of the six founder genetic backgrounds, we carried out three-way competition assays between the KanR-marked, AmpR-marked and the unmarked versions of the founders (Figure S8). Since the allele-replacement mutants carry a chromosomal *kanR* marker (see above), they were only competed against AmpR reference strains.

To start a competition assay, a query and a reference cultures were scraped from frozen stocks and inoculated into 5 mL LB-Amp or LB-Kan media as appropriate. After about 24 hours, the query and the reference cultures were mixed together in ratio 1:9 and diluted 1:10,000 into 5 mL fresh LB media. After that, the mixed culture was propagated as in the evolution experiment. To determine the relative abundances of the query and reference individuals in the mixed culture, 100 µl of appropriately diluted cultures were plated on both LB-Amp and LB-Kan plates after 24, 48 and 74 hours of competition. For some competitions, where fitness differences were particularly large or small, samples from 0 or 96 hours were also obtained. Plates were photographed after an ~24-hour incubation period (when colonies were easily visible) and colonies were automatically counted with the OpenCFU software [91]. In each competition, we estimated the fitness of the query strain relative to the reference strain by linear regression of the natural logarithm of the ratio of the query to reference strain dilution-adjusted colony counts against time. Variance was also estimated from these regressions. Replicate measurements were combined into the final estimate using the inverse variance weighting method.

Competitions between two reciprocally marked versions of the same strain represent a special case. If the two marker-carrying plasmids impose exactly the same fitness cost, our competition assay between two reciprocally marked versions of the same strain is fully symmetric, which implies that in expectation it must yield a fitness value of exactly zero. Any estimate of fitness from a finite number of measurements even in such idealized fully symmetric case will not zero. However, such deviations from zero would reflect only measurement noise rather than any biologically meaningful fitness difference. In reality, the two marker-carrying plasmids may impose slightly different fitness costs, but because the difference in the cost is detectable (see above), we still interpret deviations from zero in our fitness estimates as noise. Therefore, in competitions of reciprocally marked versions of the same strain, we set our fitness estimate to zero and use the four fitness values obtained from the replicate assays to estimate the noise variance as the average of the squared fitness value.

Growth rate assays

Strains were inoculated from frozen stock into 5 mL LB media in 15 mL culture tubes and grown overnight. After 24 hours of growth, the cultures were diluted 1:100 into fresh 5 mL of media and grown for 4 hours. They were diluted again 1:100 into 200 µl of LB in flat-bottom Costar 96 well microplates (VWR Catalog #25381-056) and grown in a Molecular Devices SpectraMax i3x

Multi-mode microplate reader at 37°C with shaking for 24 hours with absorbance measurements at 600 nm every 15 minutes. Three replicate growth measurements were conducted for each strain. Optical density data were first ln-transformed. A linear regression model was fit to all sets of 5 consecutive data points where OD was below 0.1. Growth rate for the culture was estimated as the maximal slope across all of these 5-point regressions. The mean growth rate and standard error of the mean were calculated from replicate measurements.

Genome sequencing

Whole-genome sequencing was conducted for population samples of 6 replicate populations for each of the 6 founders (36 total populations). Each population was sequenced at 11 timepoints, every 100 generations beginning at generation 0. Four lanes of 100 bp paired end sequencing was conducted at the UCSD IGM Genomics center on an Illumina HiSeq 4000 machine. The average per-base-pair coverage across all samples was 131x. Samples E1_t600, E2_t500, Y3_t600, P3_t600, P2_t800, P2_t1000 and A1_t700 yielded data inconsistent with the rest of the allele frequency trajectories from the same population, likely due to mislabelling during sample preparation. These samples were subsequently removed from our analysis.

DNA extraction and library preparation

To minimize competitive growth during handling, 100 µl of a 1:10,000 dilution of frozen stock from each sample was plated on LB agar plates and incubated at 37°C overnight. The entire plate of colonies was then scraped and used for genomic DNA extraction. DNA extractions were conducted using the Geneaid Presto mini gDNA Bacteria Kit (#GBB300) following the manufacturer's protocol. Library preparation was conducted using a modified Illumina Nextera protocol as described in [92].

Validation of variants with Sanger sequencing

43/45 variants, particularly those in loci previously annotated to be involved with translation, were validated using Sanger sequencing. Briefly, populations and timepoints containing the variant at substantial frequency were identified, and clones isolated for genomic DNA extraction, PCR and Sanger Sequencing using standard protocols. The primers used for this validation are detailed in Table S3. The two mutations that failed to validate were expected to be at relatively low frequency in their populations (17% and 38%), so additional clone sampling may be required to validate these events.

Analysis of sequencing data

Variant calling

Sequenced samples were mapped to the MG1655 reference genome (NCBI accession U00096.3) and variants were called using a custom breseq-based pipeline described in Supplementary text section 4 of Ref. [40] and kindly provided to us by Dr. Benjamin Good. Briefly, this method leverages the fact that each population was sampled multiple times across the evolution

experiment to increase our ability to distinguish real low-frequency variants from sequencing errors and other sources of noise.

The reference genome was modified with the appropriate *tufA* sequence for each genetic background used in the evolution experiment along with the removal of the *tufB* sequence, and annotation coordinates were lifted over to be consistent with the original MG1655 reference sequence using custom scripts. The modified reference genomes and annotation files are included in the github repository. The variants reported in Table S1 have been lifted back to be compatible with the original MG1655 reference genome.

Annotation

Variant annotation was conducted using the software package ANNOVAR[93]. Coding variants were established as normal, while noncoding variants were annotated as being associated with the closest gene (in either strand, in either direction) in the genome, as long as it was less than 1 kb away. As ANNOVAR is not set up to work with *E. coli* by default, the *E. coli* MG1655 nucleotide annotation was downloaded in GFF3 form from NCBI Genbank (U00096.3). Cufflinks[94] gffread tool was used to convert this file to GTF, which was then converted to GenePred by using the UCSC Genome Browser gtfToGenePred tool. The final annotation file was generated using the ANNOVAR retrieve_seq_from_fasta.pl script. The annotation file was lifted over to be compatible with each reference sequence.

Copy number variants were called manually using genome-wide coverage plots generated using samtools[95] "view" command and the R computing environment. As these variants have their frequency confounded with their copy number, only their presence/absence was noted for downstream analysis.

Filtering

We considered single nucleotide polymorphisms, short insertion/deletion and the manually identified copy number variants for further analysis. Chromosomal aberrations were ignored because breseq appears to have a high false positive rate (average of 27 "junction" calls per population across all timepoints). Variants were filtered in three successive steps. (1) Variants not identified in multiple consecutive time points were removed. (2) Variants supported by less than 10 reads across all timepoints in a given population were removed. (3) Since we observed fixation events in every population and since there should be no DNA exchange, all truly segregating variants present in a population at generation 100 must either be fixed or lost in generations 900 and 1000. Thus, we removed variants that failed to do so.

Variants that were present at an average frequency $\geq 95\%$ at generation 100 across at least 18 populations were denoted as ancestral mutations that differentiate the founder from the reference genome ($n = 10$). Variants that were not ancestral but present at $\geq 95\%$ on average across all populations derived from one founder were denoted as founder mutations ($n = 11$). These mutations were likely introduced as a byproduct of the strain engineering process. Multiallelic variants (two or more derived alleles present in a single population at the same site) were also removed as likely mapping artifacts. Finally, variants that were present at generation 100 in 11+ populations (of 36 total sequenced populations) are either mapping artifacts or pre-existing variants and were not considered further ($n = 169$, including the 10 ancestral mutations identified earlier).

Identification of adaptive mutations

The putatively adaptive mutations were identified as follows. We first identified mutations that reached at least 10% frequency, were present in at least two consecutive time points and whose frequency changed by at least 20% throughout the evolution. We then merged together such mutations within 10 bp of each other as likely being derived from a single event. This resulted in a set of candidate adaptive mutations. To identify likely adaptive mutations in this candidate set, we considered only mutations in "multihit" genes, i.e., genes with 2 or more candidate adaptive mutations.

Identification of modules in the genome

The 215 genes annotated as being associated with translation were identified using the Gene Ontology database at http://geneontology.org/ by searching for all *E. coli* K12 genes that were identified in a search for "translation OR ribosom". Similarly, the 45 genes associated with cytokinesis were identified using a search for "cytokinesis".

Statistical analyses

The expected number of mutations in multihit genes was calculated via multinomial sampling. Mutations were randomly redistributed across all genes in the *E. coli* genome controlling for variation in gene length. The average of 10,000 such randomizations was used to calculate an empirical FDR. A similar procedure was used to estimate the probability of observed as many or more TM-specific mutations by chance as we actually observed in this study.

To test whether mutations in the 7 TM-specific multi-hit loci were distributed uniformly across the six founders we first estimated the entropy of the distribution of mutations across founders for each gene. Mutations in that gene were then randomly redistributed across six founders 10,000 times, weighted by the total number of TM-specific mutations observed in each founder. An empirical *P*-value was calculated as the fraction trials with smaller than observed entropy value. These *P*-values were then corrected for multiple testing across the 7 TM-specific loci using the Benjamini-Hochberg procedure. We used the same procedure to test for significant deviations in the distributions of generic mutations across founders.

Acknowledgements

We thank members of the Kryazhimskiy and Kaçar groups, Joanna Masel, Ryan Gutenkunst, Suparna Sanyal, Grant Kinsler, Justin Meyer, and Lin Chao for input and feedback. We thank Alex Pleşa, Divjot Kaur, Emily Peñaherrera, Kevin Longoria and Lesly Villarejo for laboratory assistance. We thank Huanyu Kuo for the analysis of growth-curve data. We thank Eva Garmendia for providing the recombineering plasmids and Georg Rieckh for providing the resistance marker plasmids. We thank Benjamin Good for help with his genome sequencing data analysis pipeline. We thank Kristen Jepsen and the UCSD Institute for Genomic Medicine for sequencing services and the San Diego Supercomputing Center for providing the computational environment. BK acknowledges the support by the John Templeton Foundation (#58562 and #61239); the NASA Exobiology and Evolutionary Biology Program (#H006201406) and the NASA Astrobiology Institute (#NNA17BB05A). SK acknowledges the support by BWF Career Award at the Scientific Interface (#1010719.01), the Alfred P. Sloan Foundation (#FG-2017-9227) and the Hellman Foundation.

References

1. Simon HA. The Architecture of Complexity. Proc Am Phil Soc. 1962;106: 467–482.

2. Valentine JW, May CL. Hierarchies in Biology and Paleontology. Paleobiology. 1996;22: 23–33.

3. McShea DW. The hierarchical structure of organisms: a scale and documentation of a trend in the maximum. Paleobiology. 2001;27: 405–423.

4. Ravasz E, Somera AL, Mongru DA, Oltvai ZN, Barabási AL. Hierarchical organization of modularity in metabolic networks. Science. 2002;297: 1551–1555.

5. Mengistu H, Huizinga J, Mouret J-B, Clune J. The Evolutionary Origins of Hierarchy. PLoS Comput Biol. 2016;12: e1004829.

6. Hartwell LH, Hopfield JJ, Leibler S, Murray AW. From molecular to modular cell biology. Nature. 1999;402: C47–52.

7. Wagner GP, Pavlicev M, Cheverud JM. The road to modularity. Nat Rev Genet. 2007;8: 921–931.

8. Woese C. Molecular mechanics of translation: a reciprocating ratchet mechanism. Nature. 1970;226: 817–820.

9. Frank J. The ribosome--a macromolecular machine par excellence. Chem Biol. 2000;7: R133–41.

10. Fisher R. The genetical theory of natural selection. Oxford University Press; 1930.

11. Kacser H, Burns JA. The molecular basis of dominance. Genetics. 1981;97: 639–666.

12. Hartl DL, Taubes CH. Towards a theory of evolutionary adaptation. Genetica. 1998;102-103: 525–533.

13. Orr HA. The population genetics of adaptation: the distribution of factors fixed during adaptive evolution. Evolution. 1998;52: 935–949.

14. Welch JJ, Waxman D. Modularity and the cost of complexity. Evolution. 2003;57: 1723–1734.

15. Orr HA. The genetic theory of adaptation: a brief history. Nat Rev Genet. 2005;6: 119–127.

16. Orr HA. The distribution of fitness effects among beneficial mutations in Fisher's geometric model of adaptation. J Theor Biol. 2006;238: 279–285.

17. Waxman D. Fisher's geometrical model of evolutionary adaptation—Beyond spherical geometry. J Theor Biol. 2006;241: 887–895.

18. Martin G, Lenormand T. A general multivariate extension of Fisher's geometrical model and the distribution of mutation fitness effects across species. Evolution. 2006;60: 893–907.

19. Martin G, Lenormand T. The distribution of beneficial and fixed mutation fitness effects close to an optimum. Genetics. 2008;179: 907–916.

20. Gordo I, Campos PRA. Evolution of clonal populations approaching a fitness peak. Biol Lett.

631 2013;9: 20120239.

632 21. Tenaillon O. The Utility of Fisher's Geometric Model in Evolutionary Genetics. Annu Rev Ecol
633 Evol Syst. 2014;45: 179–201.

634 22. Hartl DL, Dykhuizen DE, Dean AM. Limits of adaptation: the evolution of selective neutrality.
635 Genetics. 1985;111: 655–674.

636 23. Lynch M. Evolutionary layering and the limits to cellular perfection. Proc Natl Acad Sci U S A.
637 2012. Available: https://www.pnas.org/content/109/46/18851.short

638 24. Nourmohammad A, Schiffels S, Lässig M. Evolution of molecular phenotypes under stabilizing
639 selection. J Stat Mech: Theory Exp. 2013;2013: P01012.

640 25. Barton NH. Linkage and the limits to natural selection. Genetics. 1995;140: 821–841.

641 26. Gerrish PJ, Lenski RE. The fate of competing beneficial mutations in an asexual population.
642 Genetica. 1998;102-103: 127–144.

643 27. Desai MM, Fisher DS. Beneficial mutation–selection balance and the effect of linkage on positive
644 selection. Genetics. 2007;176: 1759–1798.

645 28. Neher RA, Shraiman BI. Competition between recombination and epistasis can cause a transition
646 from allele to genotype selection. Proc Natl Acad Sci U S A. 2009;106: 6866–6871.

647 29. Good BH, Rouzine IM, Balick DJ, Hallatschek O, Desai MM. Distribution of fixed beneficial
648 mutations and the rate of adaptation in asexual populations. Proc Natl Acad Sci U S A. 2012;109:
649 4950–4955.

650 30. Schiffels S, Szöllosi GJ, Mustonen V, Lässig M. Emergent neutrality in adaptive asexual evolution.
651 Genetics. 2011;189: 1361–1375.

652 31. Lang GI, Botstein D, Desai MM. Genetic variation and the fate of beneficial mutations in asexual
653 populations. Genetics. 2011;188: 647–661.

654 32. Lang GI, Rice DP, Hickman MJ, Sodergren E, Weinstock GM, Botstein D, et al. Pervasive genetic
655 hitchhiking and clonal interference in forty evolving yeast populations. Nature. 2013;500: 571–574.

656 33. Kao KC, Sherlock G. Molecular characterization of clonal interference during adaptive evolution in
657 asexual populations of Saccharomyces cerevisiae. Nat Genet. 2008;40: 1499–1504.

658 34. Kvitek DJ, Sherlock G. Whole genome, whole population sequencing reveals that loss of signaling
659 networks is the major adaptive strategy in a constant environment. PLoS Genet. 2013;9: e1003972.

660 35. Herron MD, Doebeli M. Parallel evolutionary dynamics of adaptive diversification in Escherichia
661 coli. PLoS Biol. 2013;11: e1001490.

662 36. Tenaillon O, Rodríguez-Verdugo A, Gaut RL, McDonald P, Bennett AF, Long AD, et al. The
663 molecular diversity of adaptive convergence. Science. 2012;335: 457–461.

664 37. Kryazhimskiy S, Rice DP, Jerison ER, Desai MM. Global epistasis makes adaptation predictable
665 despite sequence-level stochasticity. Science. 2014;344: 1519–1522.

38. Szamecz B, Boross G, Kalapis D, Kovács K, Fekete G, Farkas Z, et al. The genomic landscape of compensatory evolution. PLoS Biol. 2014;12: e1001935.

39. Jerison ER, Kryazhimskiy S, Mitchell JK, Bloom JS, Kruglyak L, Desai MM. Genetic variation in adaptability and pleiotropy in budding yeast. Elife. 2017;6.

40. Good BH, McDonald MJ, Barrick JE, Lenski RE, Desai MM. The dynamics of molecular evolution over 60,000 generations. Nature. 2017;551: 45–50.

41. Rojas Echenique JI, Kryazhimskiy S, Nguyen Ba AN, Desai MM. Modular epistasis and the compensatory evolution of gene deletion mutants. PLoS Genet. 2019;15: e1007958.

42. Gresham D, Desai MM, Tucker CM, Jenq HT, Pai DA, Ward A, et al. The repertoire and dynamics of evolutionary adaptations to controlled nutrient-limited environments in yeast. PLoS Genet. 2008;4: e1000303.

43. Hong J, Gresham D. Molecular specificity, convergence and constraint shape adaptive evolution in nutrient-poor environments. PLoS Genet. 2014;10: e1004041.

44. Payen C, Di Rienzi SC, Ong GT, Pogachar JL, Sanchez JC, Sunshine AB, et al. The dynamics of diverse segmental amplifications in populations of Saccharomyces cerevisiae adapting to strong selection. G3 . 2014;4: 399–409.

45. Couñago R, Chen S, Shamoo Y. In vivo molecular evolution reveals biophysical origins of organismal fitness. Mol Cell. 2006;22: 441–449.

46. Chou H-H, Delaney NF, Draghi JA, Marx CJ. Mapping the fitness landscape of gene expression uncovers the cause of antagonism and sign epistasis between adaptive mutations. PLoS Genet. 2014;10: e1004149.

47. Michener JK, Neves AAC, Vuilleumier S, Bringel F, Marx CJ. Effective use of a horizontally-transferred pathway for dichloromethane catabolism requires post--transfer refinement. Elife. 2014;3: e04279.

48. Venkataram S, Dunn B, Li Y, Agarwala A, Chang J, Ebel ER, et al. Development of a Comprehensive Genotype-to-Fitness Map of Adaptation-Driving Mutations in Yeast. Cell. 2016;166: 1585–1596.e22.

49. Rodrigues JV, Shakhnovich EI. Adaptation to mutational inactivation of an essential gene converges to an accessible suboptimal fitness peak. Elife. 2019;8. doi:10.7554/eLife.50509

50. Laan L, Koschwanez JH, Murray AW. Evolutionary adaptation after crippling cell polarization follows reproducible trajectories. Elife. 2015;4. doi:10.7554/eLife.09638

51. Ramakrishnan V. Ribosome structure and the mechanism of translation. Cell. 2002;108: 557–572.

52. Williamson JR. The ribosome at atomic resolution. Cell. 2009;139: 1041–1043.

53. Melnikov S, Ben-Shem A, Garreau de Loubresse N, Jenner L, Yusupova G, Yusupov M. One core, two shells: bacterial and eukaryotic ribosomes. Nat Struct Mol Biol. 2012;19: 560–567.

54. Savir Y, Tlusty T. The ribosome as an optimal decoder: a lesson in molecular recognition. Cell. 2013;153: 471–479.

703 55. Kaçar B, Garmendia E, Tuncbag N, Andersson DI, Hughes D. Functional Constraints on Replacing
704 an Essential Gene with Its Ancient and Modern Homologs. MBio. 2017;8. doi:10.1128/mBio.01276-
705 17

706 56. Miller DL, Weissbach H. Factors involved in the transfer of aminoacyl-tRNA to the ribosome. In:
707 Petska S, Weissbach H, editors. Molecular mechanisms of protein biosynthesis. Academic Press,
708 London; 1977. pp. 323–373.

709 57. Nilsson J, Nissen P. Elongation factors on the ribosome. Curr Opin Struct Biol. 2005;15: 349–354.

710 58. Scott M, Gunderson CW, Mateescu EM, Zhang Z, Hwa T. Interdependence of Cell Growth and
711 Gene Expression: Origins and Consequences. Science. 2010;330: 1099–1102.

712 59. Tubulekas I, Hughes D. Suppression of rpsL phenotypes by tuf mutations reveals a unique
713 relationship between translation elongation and growth rate. Mol Microbiol. 1993;7: 275–284.

714 60. Schnell R, Abdulkarim F, Kálmán M, Isaksson LA. Functional EF-Tu with large C-terminal
715 extensions in an E. coli strain with a precise deletion of both chromosomal tuf genes. FEBS Lett.
716 2003;538: 139–144.

717 61. Lenski RE, Mongold JA, Sniegowski PD, Travisano M, Vasi F, Gerrish PJ, et al. Evolution of
718 competitive fitness in experimental populations of E. coli: what makes one genotype a better
719 competitor than another? Antonie Van Leeuwenhoek. 1998;73: 35–47.

720 62. Li Y, Venkataram S, Agarwala A, Dunn B, Petrov DA, Sherlock G, et al. Hidden Complexity of
721 Yeast Adaptation under Simple Evolutionary Conditions. Curr Biol. 2018;28: 515–525.e6.

722 63. Manhart M, Adkar BV, Shakhnovich EI. Trade-offs between microbial growth phases lead to
723 frequency-dependent and non-transitive selection. Proc Biol Sci. 2018;285.

724 64. Vasi F, Travisano M, Lenski RE. Long-Term Experimental Evolution in Escherichia coli. II.
725 Changes in Life-History Traits During Adaptation to a Seasonal Environment. Am Nat. 1994;144:
726 432–456.

727 65. Utnes ALG, Sørum V, Hülter N, Primicerio R, Hegstad J, Kloos J, et al. Growth phase-specific
728 evolutionary benefits of natural transformation in Acinetobacter baylyi. ISME J. 2015;9: 2221–2231.

729 66. Khan AI, Dinh DM, Schneider D, Lenski RE, Cooper TF. Negative epistasis between beneficial
730 mutations in an evolving bacterial population. Science. 2011;332: 1193–1196.

731 67. Wünsche A, Dinh DM, Satterwhite RS, Arenas CD, Stoebel DM, Cooper TF. Diminishing-returns
732 epistasis decreases adaptability along an evolutionary trajectory. Nat Ecol Evol. 2017;1: 61.

733 68. Wiser MJ, Ribeck N, Lenski RE. Long-term dynamics of adaptation in asexual populations. Science.
734 2013;342: 1364–1367.

735 69. Schoustra SE, Bataillon T, Gifford DR, Kassen R. The properties of adaptive walks in evolving
736 populations of fungus. PLoS Biol. 2009;7: e1000250.

737 70. Couce A, Tenaillon OA. The rule of declining adaptability in microbial evolution experiments. Front
738 Genet. 2015;6: 99.

739 71. Tenaillon O, Silander OK, Uzan J-P, Chao L. Quantifying organismal complexity using a population

740 genetic approach. PLoS One. 2007;2: e217.

741 72. Asai T, Zaporojets D, Squires C, Squires CL. An Escherichia coli strain with all chromosomal rRNA
742 operons inactivated: complete exchange of rRNA genes between bacteria. Proc. Natl. Acad. Sci. U.
743 S. A. 1999. pp. 1971–1976.

744 73. Dutheil JY, Jossinet F, Westhof E. Base pairing constraints drive structural epistasis in ribosomal
745 RNA sequences. Mol Biol Evol. 2010;27: 1868–1876.

746 74. Barreto FS, Burton RS. Evidence for compensatory evolution of ribosomal proteins in response to
747 rapid divergence of mitochondrial rRNA. Mol Biol Evol. 2013;30: 310–314.

748 75. Sloan DB, Triant DA, Wu M, Taylor DR. Cytonuclear interactions and relaxed selection accelerate
749 sequence evolution in organelle ribosomes. Mol Biol Evol. 2014;31: 673–682.

750 76. Shah P, McCandlish DM, Plotkin JB. Contingency and entrenchment in protein evolution under
751 purifying selection. Proc Natl Acad Sci U S A. 2015;112: E3226–35.

752 77. Starr TN, Flynn JM, Mishra P, Bolon DNA, Thornton JW. Pervasive contingency and entrenchment
753 in a billion years of Hsp90 evolution. Proc Natl Acad Sci U S A. 2018;115: 4453–4458.

754 78. Blount ZD, Lenski RE, Losos JB. Contingency and determinism in evolution: Replaying life's tape.
755 Science. 2018;362.

756 79. Orr HA. The distribution of fitness effects among beneficial mutations. Genetics. 2003;163: 1519–
757 1526.

758 80. Levy SF, Blundell JR, Venkataram S, Petrov DA, Fisher DS, Sherlock G. Quantitative evolutionary
759 dynamics using high-resolution lineage tracking. Nature. 2015;519: 181.

760 81. Chou H-H, Chiu H-C, Delaney NF, Segrè D, Marx CJ. Diminishing returns epistasis among
761 beneficial mutations decelerates adaptation. Science. 2011;332: 1190–1192.

762 82. MacLean RC, Perron GG, Gardner A. Diminishing returns from beneficial mutations and pervasive
763 epistasis shape the fitness landscape for rifampicin resistance in Pseudomonas aeruginosa. Genetics.
764 2010;186: 1345–1354.

765 83. Wei X, Zhang J. Patterns and mechanisms of diminishing returns from beneficial mutations. Mol
766 Biol Evol. 2019.

767 84. Lind PA, Tobin C, Berg OG, Kurland CG, Andersson DI. Compensatory gene amplification restores
768 fitness after inter-species gene replacements. Mol Microbiol. 2010;75: 1078–1089.

769 85. Kacar B, Ge X, Sanyal S, Gaucher EA. Experimental Evolution of Escherichia coli Harboring an
770 Ancient Translation Protein. J Mol Evol. 2017;84: 69–84.

771 86. Wagner A. Neutralism and selectionism: a network-based reconciliation. Nat Rev Genet. 2008;9:
772 965–974.

773 87. Schaper S, Johnston IG, Louis AA. Epistasis can lead to fragmented neutral spaces and contingency
774 in evolution. Proc Biol Sci. 2012;279: 1777–1783.

775 88. Newman MEJ, Engelhardt R. Effects of selective neutrality on the evolution of molecular species.

776 Proc Roy Soc B: Biological Sciences. 1998;265: 1333–1338.

777 89. Zaslaver A, Mayo AE, Rosenberg R, Bashkin P, Sberro H, Tsalyuk M, et al. Just-in-time
778 transcription program in metabolic pathways. Nat Genet. 2004;36: 486–491.

779 90. Chung CT, Niemela SL, Miller RH. One-step preparation of competent Escherichia coli:
780 transformation and storage of bacterial cells in the same solution. Proc Natl Acad Sci U S A.
781 1989;86: 2172–2175.

782 91. Geissmann Q. OpenCFU, a new free and open-source software to count cell colonies and other
783 circular objects. PLoS One. 2013;8: e54072.

784 92. Baym M, Kryazhimskiy S, Lieberman TD, Chung H, Desai MM, Kishony R. Inexpensive
785 multiplexed library preparation for megabase-sized genomes. PLoS One. 2015;10: e0128036.

786 93. Wang K, Li M, Hakonarson H. ANNOVAR: functional annotation of genetic variants from high-
787 throughput sequencing data. Nucleic Acids Res. 2010;38: e164.

788 94. Trapnell C, Roberts A, Goff L, Pertea G, Kim D, Kelley DR, et al. Differential gene and transcript
789 expression analysis of RNA-seq experiments with TopHat and Cufflinks. Nat Protoc. 2012;7: 562–
790 578.

791 95. Li H, Handsaker B, Wysoker A, Fennell T, Ruan J, Homer N, et al. The Sequence Alignment/Map
792 format and SAMtools. Bioinformatics. 2009;25: 2078–2079.

793